# Design of a re-entrant double-staggered ladder circuit for V-band coupled-cavity traveling-wave tubes*

Liu Yang(刘 洋), Xu Jin(徐 进), Lai Jian-Qiang(赖剑强), Xu Xiong(许 雄), Shen Fei(沈 飞), Wei Yan-Yu(魏彦玉), Huang Min-Zhi(黄民智), Tang Tao(唐 涛), and Gong Yu-Bin(宫玉彬)†

*National Key Laboratory of Science and Technology on Vacuum Electronics, School of Physical Electronics, University of Electronic Science and Technology of China, Chengdu* 610054, *China*

(Received 26 October 2011; revised manuscript received 13 December 2011)

The re-entrant double-staggered ladder slow-wave structure is employed in a high-power V-band coupled-cavity traveling-wave tube. This structure has a wide bandwidth, a moderate interaction impedance, and excellent thermal dissipation properties, as well as easy fabrication. A well-matched waveguide coupler is proposed for the structure. Combining the design of attenuators, a full-scale three-dimensional circuit model for the V-band coupled-cavity traveling-wave tube is constructed. The electromagnetic characteristics and the beam–wave interaction of this structure are investigated. The beam current is set to be 100 mA, and the cathode voltage is tuned from 16.8 kV to 15.8 kV. The calculation results show that this tube can produce a saturated average output power over 100 W with an instantaneous bandwidth greater than 1.25 GHz in the frequency ranging from 58 GHz to 62 GHz. The corresponding gain and electronic efficiency can reach over 32 dB and 6.5%, respectively.

**Keywords:** coupled-cavity traveling-wave tube, V band, re-entrant double-staggered ladder, slow-wave structure

**PACS:** 42.60.Da, 07.57.Hm, 41.20.Jb **DOI:** 10.1088/1674-1056/21/7/074202

## 1. Introduction

High-power millimeter-wave amplifiers with moderate bandwidths are attractive for many applications, such as high-data-rate communication, high-resolution radar, active imaging, and space applications.[1−6] Due to its outstanding combined performance in power capacity and bandwidth, the traveling-wave tube (TWT) is one of the most important millimeter-wave vacuum amplifiers.[7−14] As the core component of the TWT amplifier, the slow-wave structure (SWS) critically determines the performance of a TWT. As a full-metal structure, the coupled cavity, including the Hughes type[15−18] and the ladder type,[19−23] has been shown to have excellent power capability. Consequently, there is great interest in the study and development of high-power millimeter-wave coupled-cavity traveling-wave tube (CCTWT). For example, the Hughes-type coupled cavity has been used to develop a 75 W 59–64 GHz TWT for inter-satellite communications.[16] However, when the operating frequency increases to be within the shorter millimeter-wave band, the Hughes-type coupled-cavity circuit will be expensive and difficult to fabricate by the conventional machining because of the extremely small manufacturing tolerances. In order to solve this problem, the ladder-type coupled cavity was proposed by James and Kolda.[19] The ladder circuit can be easily fabricated from a single copper block, through which the cumulative errors of the stacked cavities can be eliminated. Then, the circuit can achieve the extremely tight tolerances required to maintain the synchronism between the electron beam and the radio frequency (RF) waves. Meanwhile, among the ladder coupled cavities, the double-staggered ladder has the widest bandwidth.[19,20] In order to develop a high-power V-band TWT with a moderate bandwidth for inter-satellite communications, the re-entrant double-staggered ladder-coupled cavity is adopted because of its wide frequency bandwidth, moderate interaction impedance, and excellent thermal dissipation properties, as well as its easy fabrication.

In this paper, we present the design and the anal-

*Project supported by the National Science Fund for Distinguished Young Scholars of China (Grant No. 61125103), the Vacuum Electronics National Lab Foundation, China (Grant No. 9140C050101110C0501), and the Fundamental Research Funds for the Central Universities, China (Grant Nos. ZYGX2009Z003 and ZYGX2010J054).

†Corresponding author. E-mail: ybgong@uestc.edu.cn

© 2012 Chinese Physical Society and IOP Publishing Ltd

ysis of a re-entrant double-staggered ladder circuit for V-band CCTWT by utilizing HFSS[24] and the CST studio suite.[25,26] The rest of this paper is organized as follows. In Section 2, the model of the re-entrant double-staggered ladder-coupled cavity is described in detail. High frequency properties, such as dispersion characteristics and beam–wave interaction impedance, are studied and optimized. In Section 3, a well-matched waveguide coupler is proposed for the re-entrant double-staggered ladder circuit. The transmission characteristics of this ladder circuit are obtained. In Section 4, we perform the beam–wave interaction simulation in the presence of an electron beam and predict the operating characteristics of the V-band CCTWT, such as saturated average output power, gain, and electronic efficiency. In Section 5, a Conclusion and a description of the future work are given.

## 2. Slow-wave structure design

Figure 1 shows the model of the re-entrant double-staggered ladder- coupled cavity. The coordinate system used in the simulation is a rectangular one $(x, y, z)$, with a positive $z$ axis running along the axis of the beam tunnel. The cavities have square-shaped cross sections $(w \times w)$. Unlike the traditional double-staggered ladder-coupled cavity proposed by James and Kolda,[19] we adopt a re-entrant ferrule to concentrate the axial electric fields in the beam interaction gap, as shown in Fig. 1(a). Figure 1(b) shows the alternating cavity wall cross-sectional views at the $A$–$A'$ and the $B$–$B'$ planes. The circuit is fabricated by machining two coupling slots 180° apart from the beam axis in each wall between the cavities. And the slot positions are rotated through 90° about the beam tunnel axis on the successive walls. Compared with the Hughes-type coupled–cavity circuit, the ladder circuit can be more easily fabricated with extremely tight tolerances.

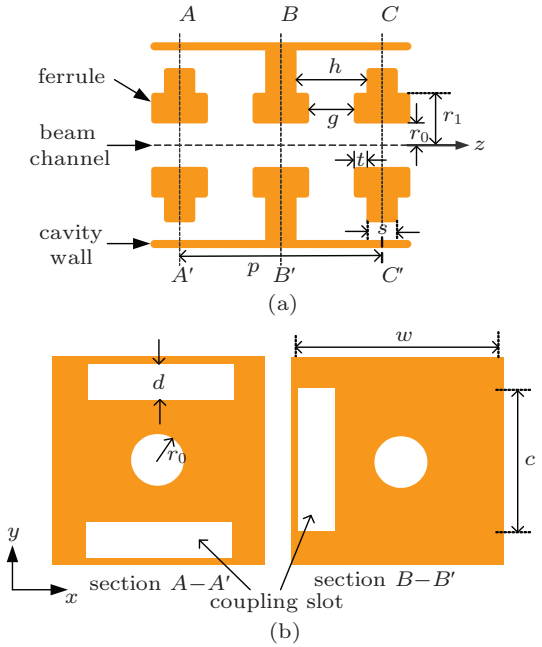



**Fig. 1.** (colour online) Dimensional parameters of the re-entrant double-staggered ladder-coupled cavity: (a) cutaway view in the direction of the beam tunnel and (b) cross-sectional views at $A$–$A'$ and $B$–$B'$ planes.

Figure 2 shows the electric field distribution of the fundamental mode for the re-entrant double-staggered ladder-coupled cavity. This structure has a strong symmetric axial electric field along the electron beam propagation direction, which is essential to the beam–wave interaction of the TWT. Meanwhile, we can also see that the re-entrant ferrule of the cavity concentrates the axial electric field in the beam interaction gap, which can enhance the beam–wave interaction efficiency.

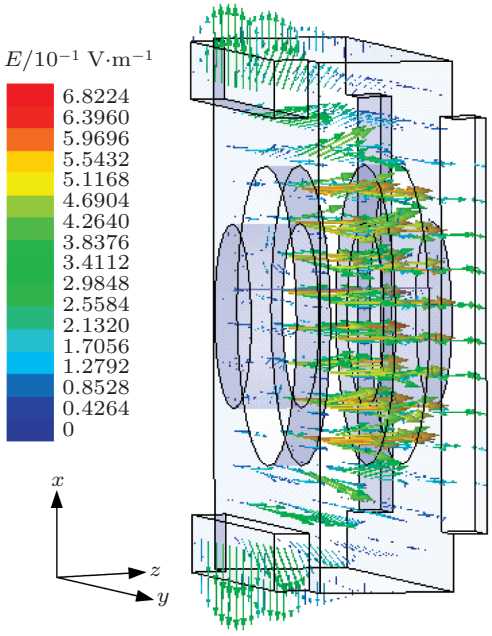



**Fig. 2.** (colour online) Electric field distribution of the fundamental mode for the re-entrant double-staggered ladder-coupled cavity.

The high frequency properties of this structure are simulated by using HFSS,[24] which include the dispersion characteristics and the beam–wave interaction impedance. Since the slow-wave structure is periodic, the simulation can be carried out just in one pitch. By employing the master and slave boundary condition in the eigenmode solver,[27] the simulation can be conducted and optimized in an efficient and accurate way. The typical optimized structural parameters are listed in Table 1. As shown in Fig. 3(a), this type of circuit is a fundamental backward wave

circuit, and the electron beam interacts with the first spatial harmonic. The phase shift and the cavity period determine the circuit wave velocity, which in turn determines the beam voltage to be approximately 16 kV for the central frequency of 60 GHz required for the synchronized interaction with the electron beam. Since the dispersion of this structure is fairly strong, the cathode voltage is tuned to acquire a wider operating bandwidth in our design. Changing the cathode voltage from 16.8 kV to 15.8 kV results in the synchronization of the electron beam with the RF wave over a frequency band from 58 GHz to 62 GHz, as shown in Fig. 3(b). Meanwhile, as this ladder circuit has a wide cold bandwidth, the high impedance band-edge frequencies, especially the upper band-edge frequency at $2\pi$, are far away from synchronism with the electron beam, the risk of band-edge oscillations will be avoided.[28]

**Table 1.** Optimized structural parameters.

| Parameter | Value/mm |
|---|---|
| Cavity ($w \times w$) | $2.22 \times 2.22$ |
| Coupling slot ($c \times d$) | $1.74 \times 0.24$ |
| Cavity height ($h$) | 0.568 |
| Cavity gap ($g$) | 0.278 |
| Slot height ($s$) | 0.29 |
| Ferrule height ($t$) | 0.145 |
| Ferrule radius ($r_1$) | 0.63 |
| Beam tunnel radius ($r_0$) | 0.38 |
| Period length ($p$) | 1.716 |

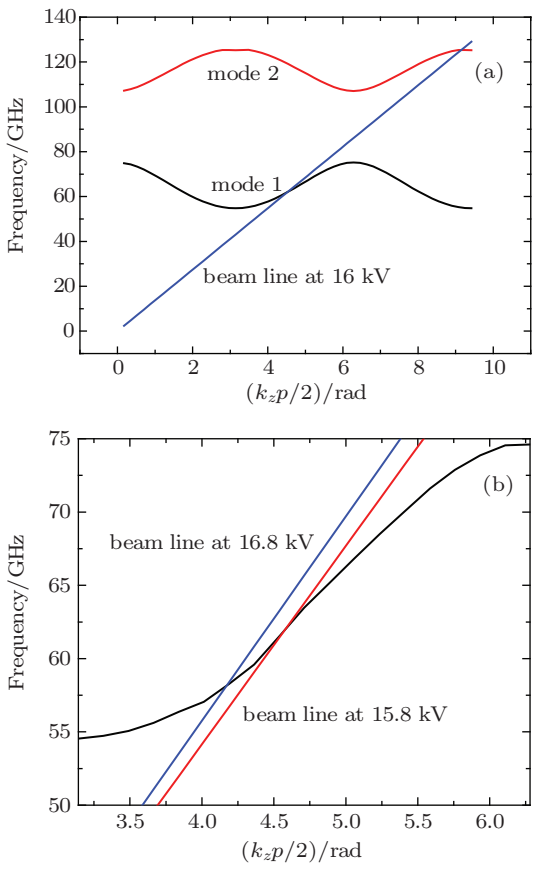



**Fig. 3.** (colour online) (a) Dispersion characteristics with synchronous beam voltage lines. (b) Voltage-tuned bandwidth.

As a measure of the interaction strength between the electron beam and the RF wave, the average interaction impedance calculated for the first spatial harmonic is given in Fig. 4, which is calculated in the central area of the circular beam tunnel with a radius of 0.19 mm. The impedance is greater than 4.5 Ω in the frequency range from 58 GHz to 62 GHz, which indicates that the structure can support fairly strong beam–wave interaction.

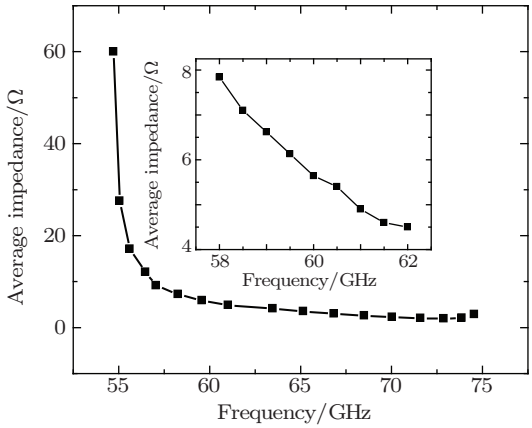



**Fig. 4.** Average interaction impedance versus frequency. The inset shows the details of the transition.

## 3. Input/output coupler design

A good coupler between the coupled-cavity circuit and the waveguide is important for improving tube efficiency, gain, and stability over the required bandwidth. It is also conducible to preventing the band-edge oscillation at the upper cut-off frequency of the cavity mode.[30] Therefore, the design and the optimization of the waveguide coupler for the coupled cavity are important parts of the CCTWT design. However, the coupled cavity is inherently a three-dimensional structure, and the design of broadband low-VSWR couplers is a complicated process. The available literature in this respect is relatively rare and just limited to the case of Hughes-type structure.[29,30]

In this section, a well-matched input/output coupler with a simple structure for the re-entrant double-staggered ladder CCTWT is proposed. It is composed of three components, i.e., a flat rectangular waveguide,

a transition section, and a waveguide transformer, as shown in Fig. 5(a). The flat rectangular waveguide, with a wide side length of 3.795 mm (the same as that of the standard waveguide WR-15) and a narrow side length of $h$ (equal to the cavity height, 0.568 mm), is inserted into the cavity from the direction of the coupling slot. From the waveguide to the transition section, there are mainly two categories of free parameters, namely the cavity and the slot parameters, to be varied to adjust the VSWR within the range of interest when the flat rectangular waveguide is fixed. As the cavity structure parameters are determined mainly by the operating voltage and frequency, they will not be varied here. We just change the size of the slot ($c \times d$) with the other structure parameters kept constant. In our design, length $c$ and width $d$ of the slot are gradually increased to match the input/output flat rectangular waveguide. And then a gradual transition section between the main SWS section and the flat rectangular waveguide within the length of two periods is formed. Meanwhile, a three-step waveguide transformer from the input/output flat rectangular waveguide (0.568 mm×3.795 mm) to the standard waveguide WR-15 (1.88 mm×3.795 mm) is also designed here.[31]

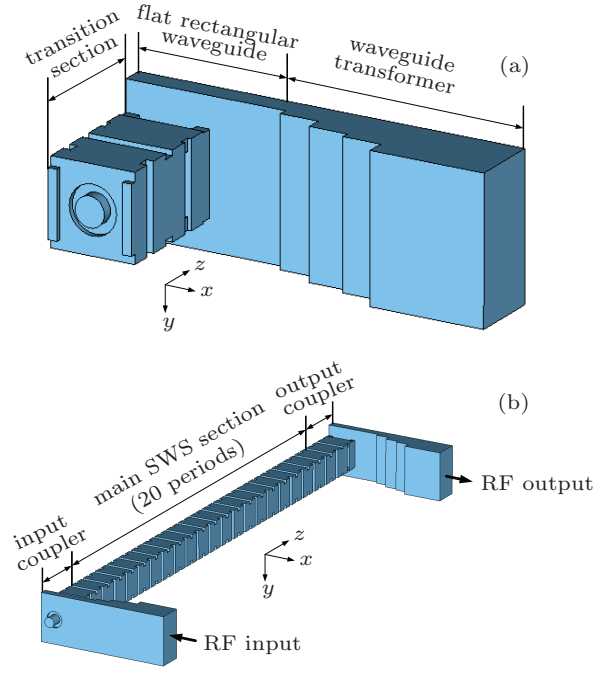



**Fig. 5.** (colour online) (a) Coupler model and (b) transmission model of the re-entrant double-staggered ladder circuit.

The transmission model of the coupler-cavity circuit including 20 periods of main SWS section and input/output coupler is presented in Fig. 5(b). The boundary is set as copper with an effective conductivity of $3.5\times10^7$ S/m considering the surface roughness.[15,32] By using the transient solver in the CST Microwave Studio[25] and sweeping the free parameters, the optimal coupler for the structure is obtained. The transmission characteristics are shown in Fig. 6. The reflection parameter $S_{11} < -16$ dB and the VSWR<1.4 in the frequency range from 58 GHz to 62 GHz are obtained. This result illustrates that the designed input/output coupler is well matched to the circuit over a wide frequency range.

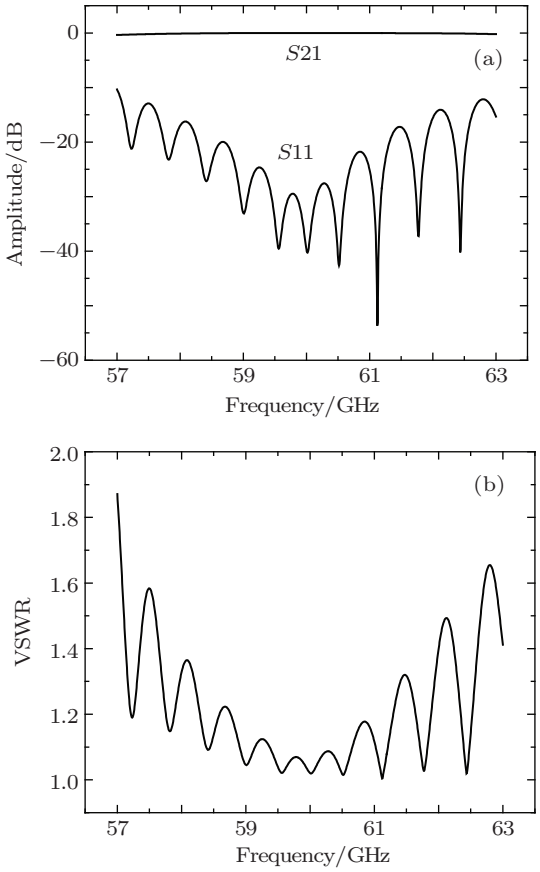



**Fig. 6.** (a) Parameter $S$ and (b) VSWR of the re-entrant double-staggered ladder circuit.

## 4. Particle-in-cell simulations

In this section, a full-scale three-dimensional (3D) circuit model for the V-band CCTWT is presented. And the particle-in-cell simulations are carried out to investigate the beam dynamics of the CCTWT using the PIC solver in the CST Particle Studio.[26] The dimensional parameters are listed in Table 1. In order to obtain a large gain and suppress the oscillation caused by reflection, the whole interaction circuit is divided into two sections by attenuators.[33] As shown in Fig. 7, the first section consists of 23 periods, and the second one is composed of 31 periods.

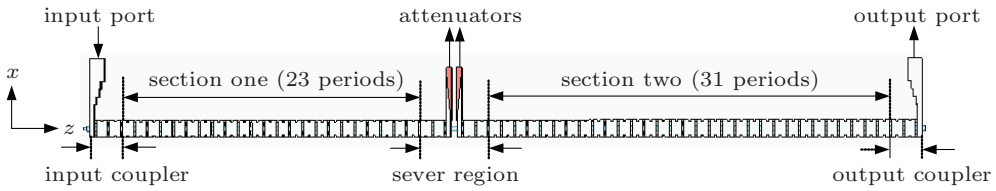



**Fig. 7.** (colour online) Full-scale 3D circuit model for the V-band CCTWT.

Before performing the particle-in-cell simulations, the transmission characteristics of the first section circuit including the attenuator are investigated, as shown in Fig. 8. The attenuator adopts a long linear taper to provide a good match and sufficient attenuation.[34] In our simulation, the length of the attenuator is four periods, and the lossy ceramic material (80% BeO and 20% SiC) with a loss tangent of 0.3 and a relative permittivity of 11.5[35] is used for the attenuator. The transmission characteristics of this circuit with the optimized attenuators are obtained and shown in Fig. 9. The $S_{11}$ is almost below $-15$ dB and $S_{21}$ keeps below $-30$ dB throughout the bandwidth from 58 GHz to 62 GHz.

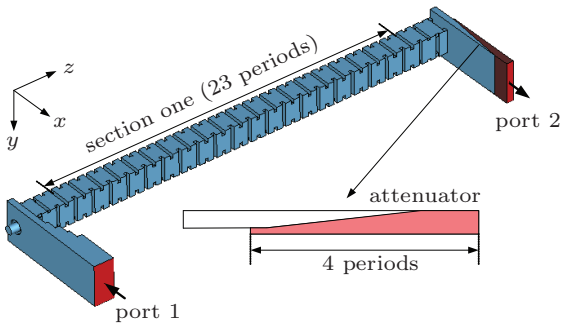



**Fig. 8.** (colour online) Three-dimensional model of the re-entrant double-staggered ladder circuit with an attenuator.

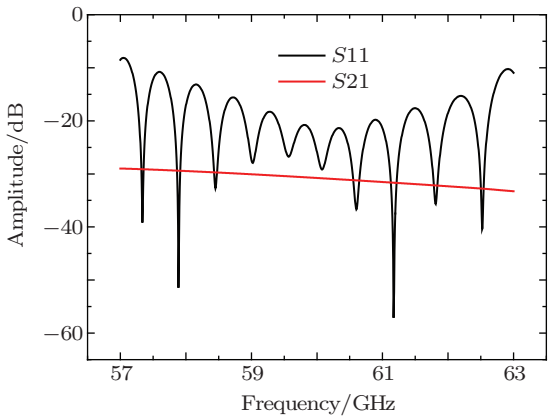



**Fig. 9.** (colour online) Transmission characteristics of the re-entrant double-staggered ladder circuit given in Fig. 8.

In our simulation, we assume that the circular beam has a radius of 0.19 mm with a current of 100 mA, corresponding to a beam filling factor of 50% with a current density of 88 A/cm$^2$. And a samarium-cobalt periodic permanent magnetic (PPM) field with an amplitude of 0.3 T and a period of 9.5 mm is used to confine the electron beam. The boundary is also specified as copper with an effective conductivity of $3.5\times10^7$ S/m.

The typical simulation results at 60 GHz are exhibited in Figs. 10–12. The cathode voltage is set to be 16.2 kV, and the input driven signal with a power of 45 mW is applied. Figure 10 shows the frequency spectra of input, output, and reflected signals. As for the output signal, the spectrum is relatively pure. Although the higher harmonics are also aroused, the amplitudes are much lower than that of the operating frequency at 60 GHz. Meanwhile, it can be learnt that the reflected power is well below the input power, which implies that the oscillation is unlikely to occur.

As shown in the inset of Fig. 11, the accelerating and the retarding electrons are periodically arranged along the longitudinal direction, which demonstrates a good beam–wave energy exchange. Figure 11 shows the phase momentum plot of the bunched electron beam along the longitudinal direction when the electron dynamic system is in the steady state. As the electron beam propagates along the circuit, most of the electrons are decelerated and lose their kinetic energies at the end of the circuit. Consequently, the lost kinetic energy of the electron beam is transferred to the high frequency electromagnetic field. Then, the amplification of the input signal is observed, as shown in Fig. 12. The output signal becomes stable at 140 W with an electronic efficiency of 8.64% and a gain of 34.93 dB after 2.8 ns, and no oscillation occurs.

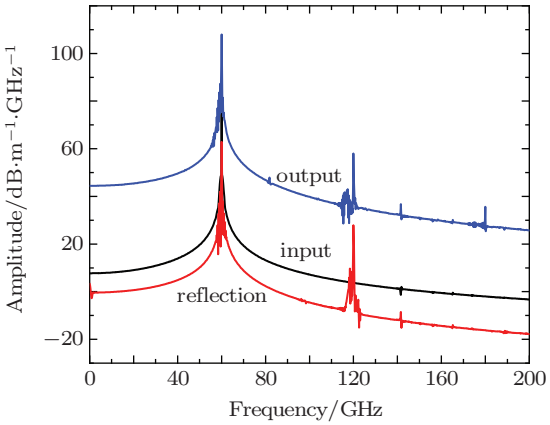



**Fig. 10.** (colour online) Frequency spectra of input, output, and reflected signals at 60 GHz.

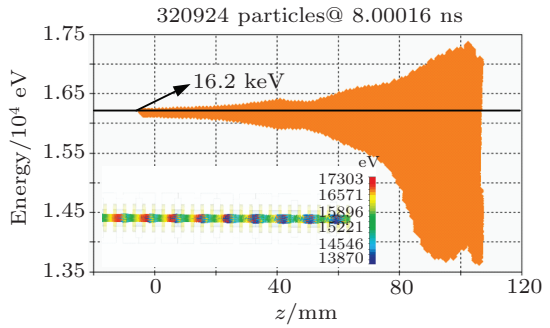



**Fig. 11.** (colour online) Phase momentum ($p_z$) plot of the bunched electron beam at 60 GHz, the inset shows the electron bunching phenomenon around the end of the SWS.

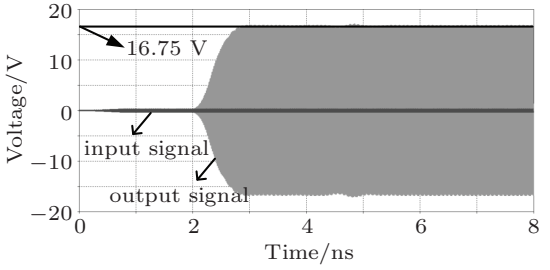



**Fig. 12.** Input and output signals at 60 GHz.

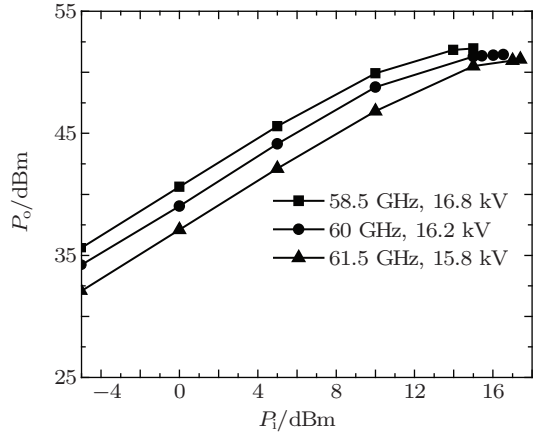



**Fig. 13.** Power transfer curves across the voltage-tuned bandwidth.

To find the saturation, the power transfer curves at three typical frequencies that span the voltage tuned bandwidth of the TWT are shown in Fig. 13. At each frequency, the TWT can be driven up to a saturated average output power of over 100 W (50 dBm). The saturated gain of the TWT decreases with the increase of the working frequency, which can be explained by the frequency variation of the interaction impedance illustrated in Fig. 4.

In order to obtain the instantaneous bandwidth of this TWT, the curves of saturated output power versus frequency for three fixed beam voltages, i.e., 16.8 kV, 16.2 kV, and 15.8 kV, are shown in Fig. 14. The voltage tuned TWT can produce a saturated output power over 100 W in the frequency range from 58 GHz to 62 GHz. The corresponding gain and electronic efficiency can reach over 32 dB and 6.5%, respectively. Changing the cathode voltage results in the synchronization of the electron beam and the RF waves over different frequency bands, which means that the saturated output power can be tuned to different frequencies by changing the cathode voltage. Meanwhile, when it operates at a fixed cathode voltage, the TWT can have an instantaneous bandwidth greater than 1.25 GHz. The typical operating parameters for the ladder CCTWT are summarized in

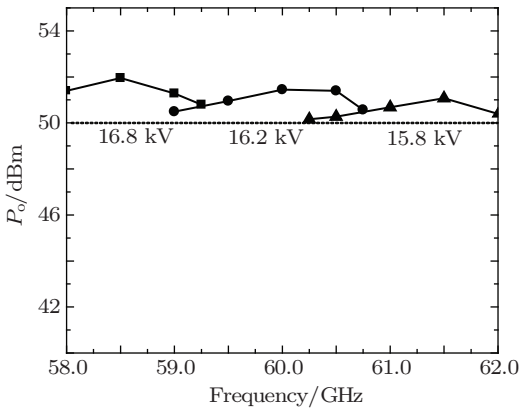



**Fig. 14.** 100 W operations in three voltage-tuned instantaneous bands.

**Table 2.** Operating parameters for the CCTWT.

| Parameter | Value |
|---|---|
| Frequency | 58–62 GHz |
| Beam current | 100 mA |
| Cathode voltage | 16.8–15.8 kV |
| Circuit section | 2 |
| Saturated output power | $>$ 100 W |
| Saturated gain | $>$ 32 dB |
| Instantaneous bandwidth | $>$ 1.25 GHz |

Table 2. Compared with the Hughes-type V-band CCTWT,[16] our designed CCTWT has the performance that is more competitive in power capability. And more importantly, the ladder-type CCTWT can be easily fabricated and assembled with extremely tight tolerances.

## 5. Conclusion

The re-entrant double-staggered ladder SWS is employed as the RF circuit for the V-band CCTWT and has been proved to possess outstanding cold and hot performances. An input/output coupler is proposed for the structure, which can be well matched to the structure over a wide frequency range. As far as we know, this is the first time that the CST 3D simulation has been conducted for a full-scale V-band CCTWT. The simulation results show that the tube can produce a saturated output power over 100 W with a gain over 32 dB at the frequencies ranging from 58 GHz to 62 GHz when the cathode voltage is tuned from 16.8 kV to 15.8 kV. And when it operates at a fixed cathode voltage, the TWT can have an instantaneous bandwidth greater than 1.25 GHz. Compared with the Hughes-type coupled cavity, our designed CCTWT has the performance that is more competitive in power capability. More importantly, the ladder-type CCTWT can be easily fabricated and assembled with extremely tight tolerances. Therefore, it is a competing high-power millimeter-wave amplifier.

Moreover, our design scheme including the proposed input/output coupler will have significant reference values for engineers to develop the millimeter-wave CCTWT. Future work will be concentrated on the design of the electron optical system, RF windows, etc. And the experimental study of this CCTWT will be carried out.

## References


[1] Feng J J, Hu Y F, Cai J, Wu X P and Tang Y 2010 *Vacuum Electronics* **52** 27 (in Chinese)

[2] Zhong K, Yao J Q, Xu D G, Zhang H Y and Wang P 2011 *Acta Phys. Sin.* **60** 034210 (in Chinese)

[3] Guo Z, Fan F, Bai J J, Niu C and Chang S J 2011 *Acta Phys. Sin.* **60** 074218 (in Chinese)

[4] Hao B L, Xiao L, Liu P K, Li G C, Jiang Y, Yi H X and Zhou W 2009 *Acta Phys. Sin.* **58** 3118 (in Chinese)

[5] Du C H, Liu P K and Xue Q Z 2010 *Acta Phys. Sin.* **59** 4611 (in Chinese)

[6] Kornfeld G K, Bosch E, Gerum W and Fleury G 2001 *IEEE Trans. Electron Devices* **48** 68

[7] Zhang C Q, Cong Y B, Wei Y Y and Wang W X 2010 *Acta Phys. Sin.* **59** 6653 (in Chinese)

[8] He J, Wei Y Y, Gong Y B and Wang W X 2010 *Acta Phys. Sin.* **59** 2843 (in Chinese)

[9] He J, Wei Y Y, Gong Y B and Wang W X 2010 *Acta Phys. Sin.* **59** 6659 (in Chinese)

[10] He J, Wei Y Y, Gong Y B and Wang W X 2011 *Chin. Phys.* B **20** 054102

[11] Gao X, Yang Z Q, Cao W P and Jiang Y N 2011 *Chin. Phys.* B **20** 030703

[12] Jiang B, Zhang Y J, Zhou W J, Chen W, Liu A J and Zheng W H 2011 *Chin. Phys.* B **20** 024208

[13] Hu Y T, Xiao X, Li Z Y, Li Y T, Fan Z C, Han W H, Yu Y D and Yu J Z 2011 *Chin. Phys.* B **20** 074208

[14] Huang J, Dong J R, Yang H, Zhang H Y, Tian C and Guo T Y 2011 *Chin. Phys.* B **20** 060702

[15] Wilson J D and Kory C L 1995 *IEEE Trans. Electron Devices* **42** 2015

[16] Wilson J D, Ramins P and Force D A 1991 *International Electron Devices Meeting*, December 8–11, 1991 Washington D.C., USA, p. 585

[17] Curnow H J 1965 *IEEE Trans. Microw. Theory Tech.* **13** 671

[18] Freund H P, Antonsen T M Jr, Zaidman E G, Levush B and Legarra J 2002 *IEEE Trans. Plasma Sci.* **30** 1024

[19] James B G and Kolda P 1986 *International Electron Devices Meeting*, December 7–10, 1986 Los Angeles, USA, p. 494

[20] Gong Y B, Mo Y L, Zhou Y D and Zhou X L 1996 *Int. J. IR/MM Waves* **17** 796

[21] Choi J J and Kim H J 2011 *Journal of Infrared, Millimeter and Terahertz Waves* **32** 1

[22] Legarra J R, Cusick J, Begum R, Kolda P and Cascone M 2005 *IEEE Trans. Electron Devices* **52** 665

[23] Kim H J, Kim H J and Choi J J 2009 *IEEE Trans. Electron Devices* **56** 149

[24] *Ansoft HFSS User's Reference*, available at: http://www.ansoft.com.cn/

[25] *CST MWS Tutorials*, available at: http://www.cst-china.cn/

[26] *CST PS Tutorials*, available at: http://www.cst-china.cn/

[27] Booske J H, Converse M C, Kory C L, Chevalier C T, Gallagher D A, Kreischer K E, Heinen V O and Bhattacharjee S 2005 *IEEE Trans. Electron Devices* **52** 685

[28] Nusinovich G S, Sinitsyn O V and Antonsen T M Jr 2010 *Phys. Rev.* E **82** 046404

[29] Kageyama T 2002 *IEEE International Vacuum Electronics Conference*, April 23–25, 2002 Californis, USA, p. 102

[30] Christie V L, Sumathy M, Kumar L and Prasad S 2010 *IEEE International Vacuum Electronics Conference*, May 18–20, 2010 Monterey, USA, p. 263

[31] Young L 1962 *IRE Trans. Microw. Theory Tech.* **10** 339

[32] Tischer F J 1976 *IEEE Trans. Microw. Theory Tech.* **24** 853

[33] Srivastave V and Carter R G 1991 *IEE Proceedings-H* **138** 55

[34] Kory C L and Ives R L 2006 *IEEE International Vacuum Electronics Conference*, April 25–27, 2006 Monterey, USA, p. 447

[35] Cai J, Feng J J, Wu X P, Hu Y F, Qu B, Huang M G and Ma S Y 2007 *IEEE International Vacuum Electronics Conference*, May 15–17, 2007 Kitakyushu, Japan, p. 1